Porous Upconversion Nanostructures as Bimodal Biomedical Imaging Contrast Agents

*Ziqing Du[1], Abhishek Gupta[2], Christian Clarke[1], Matt Cappadana[1], David Clases[3], Deming Liu[1], Zhuoqing Yang[4], Shawan Karan[5], William S. Price[2], Xiaoxue Xu[1]**

[1]Institute for Biomedical Materials and Devices, Faculty of Science, University of Technology Sydney, NSW, 2007, Australia

[2]Nanoscale Organisation and Dynamics Group, School of Science, Western Sydney University, NSW, 2751, Australia

[3]Elemental Bio-Imaging Facility, School of Mathematical and Physical Sciences, University of Technology Sydney, NSW, 2007, Australia

[4]National Key Laboratory of Science and Technology on Micro/Nano Fabrication, School of Electronic Information and Electrical Engineering, Shanghai Jiao Tong University, Shanghai, 200240, P. R. China

[5]Office of Technical Support Services, Western Sydney University, NSW, 2751, Australia

Corresponding author: xiaoxuehelen.xu@uts.edu.au

1 1. Experimental and Materials

2 1.1 Materials and Chemicals

3 Yttrium chloride hexahydrate ($YCl_3 \cdot 6H_2O$, 99.99%), ytterbium chloride hexahydrate
4 ($YbCl_3 \cdot 6H_2O$, 99.998%), erbium chloride hexahydrate ($ErCl_3 \cdot 6H_2O$, 99.9%), gadolinium
5 chloride hexahydrate ($GdCl_3 \cdot 6H_2O$, 99%), sodium hydroxide (NaOH, 98%), ammonium fluoride
6 (NH_4F, 99.99%), oleic acid (OA, 90%), 1-octadecene (ODE, 90%), KOH (reagent grade, 90%)
7 and hydrochloric acid (HCl, 37%) were purchased from Sigma-Aldrich. All reagents were used
8 as received without further purification.

9 1.2 Nanomaterials synthesis

10 *Core upconversion nanoparticles synthesis of $NaYF_4$: 20%Yb, 1%Er:* The $NaYF_4$: 20%Yb,
11 1%Er. The typical synthesis procedure is as follows:[1] Lanthanide chloride in total 1 mmol,
12 including YCl_3, $YbCl_3$ and $ErCl_3$, were dissolved in methanol base at a molar ratio of 79:20:1
13 and then mixed with 6 ml oleic acid and 15 ml octadecene. In order to remove methanol and
14 dissolve the lanthanide salts, the mixture was heated to 150 °C for 30 minutes. After cooling to
15 room temperature, 4 mmol sodium hydroxide (NaOH) and 2.5 mmol ammonium fluoride (NH_4F)
16 in methanol solution was added and stirred for another 30 minutes. The mixture was heated at
17 90 °C for 30 minute and 150 °C for a further 10 minutes to evaporate the water and methanol.
18 Subsequently, the reaction solution was heated to 300 °C for 90 minutes. Controlling the heating
19 rate allows various sized nanoparticles to be synthesised,[2] large UCNPs were formed with a 6
20 min heating rate, small UCNPs were formed with a 12 min heating rate. The nanoparticles were
21 washed using oleic acid, cyclohexane, methanol and ethanol mixture after the reaction solution
22 was cooled to room temperature. Samples were dispersed in cyclohexane for further use.

Core-shell nanostructure synthesis of $NaYF_4$: 20%Yb,1%Er@$NaYF_4$: 30% Gd: The core-shell structure was fabricated using a hot injection method [1]. Before the injection, the $NaYF_4$:30%Gd shell precursor was prepared with YCl_3 and $GdCl_3$ salts dissolved in oleic acid and octadecene with NaOH and NH_4F. Core nanoparticles (0.2 mmol) dispersion in cyclohexane was added to 3 ml oleic acid and 8 ml octadecene and heated to 150 °C for removing cyclohexane and possible water and then the reaction solution was heated up to 300 °C. Shell precursor solution was injected into the core dispersion at a constant speed of 0.1 ml/min. Upon completion of the injection, the mixture solution was kept at 300 °C for 10 min and then cooled to room temperature. The precipitate was washed using the mixture of oleic acid, cyclohexane, methanol and ethanol, and dispersed in cyclohexane for characterization and porous treatment.

Core-porous shell nanostructures synthesis of $NaYF_4$: 20%Yb, 1%Er@ $NaYF_4$: 30% Gd: Porous treatment followed our previous work [1]. Typically, 5 mmol potassium hydroxide in methanol was added in 3 ml oleic acid and 8 ml octadecene and the methanol was evaporated at 120 °C. The temperature was decreased to 80 °C before 0.2 mmol core-shell UCNPs were added. The resulting mixture was heated to 120 °C and held for 10 mins, and then increased to 300 °C and maintained there for 10-15 min. The resulted precipitates were washed and stored as described for the core and core-shell UNCPs.

1.3 Characterizations and Measurements

TEM images of all nanoparticles were recorded with a FEI Tecnai T20 transmission electron microscope. The diameter of the nanoparticles was determined, counted and graphed with ImageJ 1.50I software. The Energy Dispersive X-Ray spectroscopy (elemental mapping) of nanoparticles was performed using a JEOL JEM-ARM200f transmission electron microscope and the result was processed with Noran System 7 EDS software.

Crystal phase analysis of nanoparticles was applied using a Bruker D8 Discover A25 X-ray diffractometer with Cu Kα1 radiation (40 kV, 40 mA, λ=0.15406 nm). The results were compared with PDF-4+2019 RDB database to identify the crystal phase and structure.

Photoluminescent spectra were recorded of the cyclohexane dispersions of the core, core-shell and core-porous shell UCNPs using an Ocean Optics QE65000 spectrometer at 980 nm. The emission intensity was normalized to the Er^{3+} doping concentration following quantification by ICP-MS. The single UCNPs emission performances were characterized using a homebuilt Scanning Confocal Microscopy as described elsewhere in previous work.[3] All experiments were performed with a power density of 2 MW/cm^2.

ICP-MS quantification for the Gd^{3+} concentration was conducted as the following procedure. The exact concentrations of Gd^{3+} in the stock solutions of UCNPs were determined using inductively coupled plasma-mass spectrometry (ICP-MS) on a NexION 300X ICP-MS instrument (PerkinElmer, USA). All the UCNPs were washed using 0.1 M HCl solution gently for 0.5 h to remove the OA on the surface and the UCNPs were converted to hydrophilic surfaces. Since it is known that the digestion of inorganic nanoparticles (especially fluoride) can be difficult, inevitably leading to underestimation of the metal ion concentration (and, in turn, over estimation of relaxivity values),[4-5] two different digestion procedures were followed and the results compared. In one protocol, predetermined amounts of the UCNPs dispersions were added directly to 2% HNO_3 and the dilutions were left at room temperature for a week. In the other protocol, predetermined amounts of UCNPs dispersions were added to 70% concentrated nitric acid and left to digest overnight. The samples were then heated at 170 °C for ~5 h to complete digestion and evaporate the acid using a SPB 15-108 heating block (PerkinElmer, USA). The dry digested sample was diluted with 2% HNO_3 and then transferred to 15 mL vials made of PP

before conducting ICP-MS measurements. A calibration curve was obtained by analysing serial dilutions of a mixed element ICP-MS standard containing a known concentration of Gd^{3+}. Accuracy was confirmed by the analysis of a commercial MRI contrast agent with a known concentration of Gd^{3+}.

The results obtained using the two digestion protocols were found to be in agreement with each other. Therefore, the average of the values from both approaches were used in relaxivity determination.

Relaxivity Measurements: Four dilutions were prepared of each sample by adding Milli-Q water. Longitudinal (T_1) and transverse (T_2) NMR relaxation times of the dilutions were measured at 25 °C on two spectrometers: a Magritek Spinsolve 43 MHz (1 T) benchtop spectrometer (Magritek, New Zealand) and a Bruker Avance 500 MHz (11.7 T) spectrometer (Bruker Biospin, Germany). T_1 and T_2 measurements were performed using inversion recovery[6] and CPMG pulse[7-8] sequences, respectively. Samples were placed in straight capillary tubes (529-D, Wilmad LabGlass, USA), which were flame sealed and then placed in 5-mm NMR tubes (528-PP-7, Wilmad Lab Glass, USA). All samples were equilibrated for 10 min. at the set temperature prior to conducting relaxation measurements. All NMR experiments were carried out without field frequency locking. The recycle delay was set to $\geq 5T_1$ and the signal was averaged over four scans for both inversion recovery and CPMG measurements. All data fitting for the T_1 and T_2 measurements was performed using OriginPro 2018 (OriginLab, USA). The relaxivity was calculated from the slope of the plots of inverse relaxation times versus Gd^{3+} concentration (as determined from ICP-MS).

2. Supplementary Results

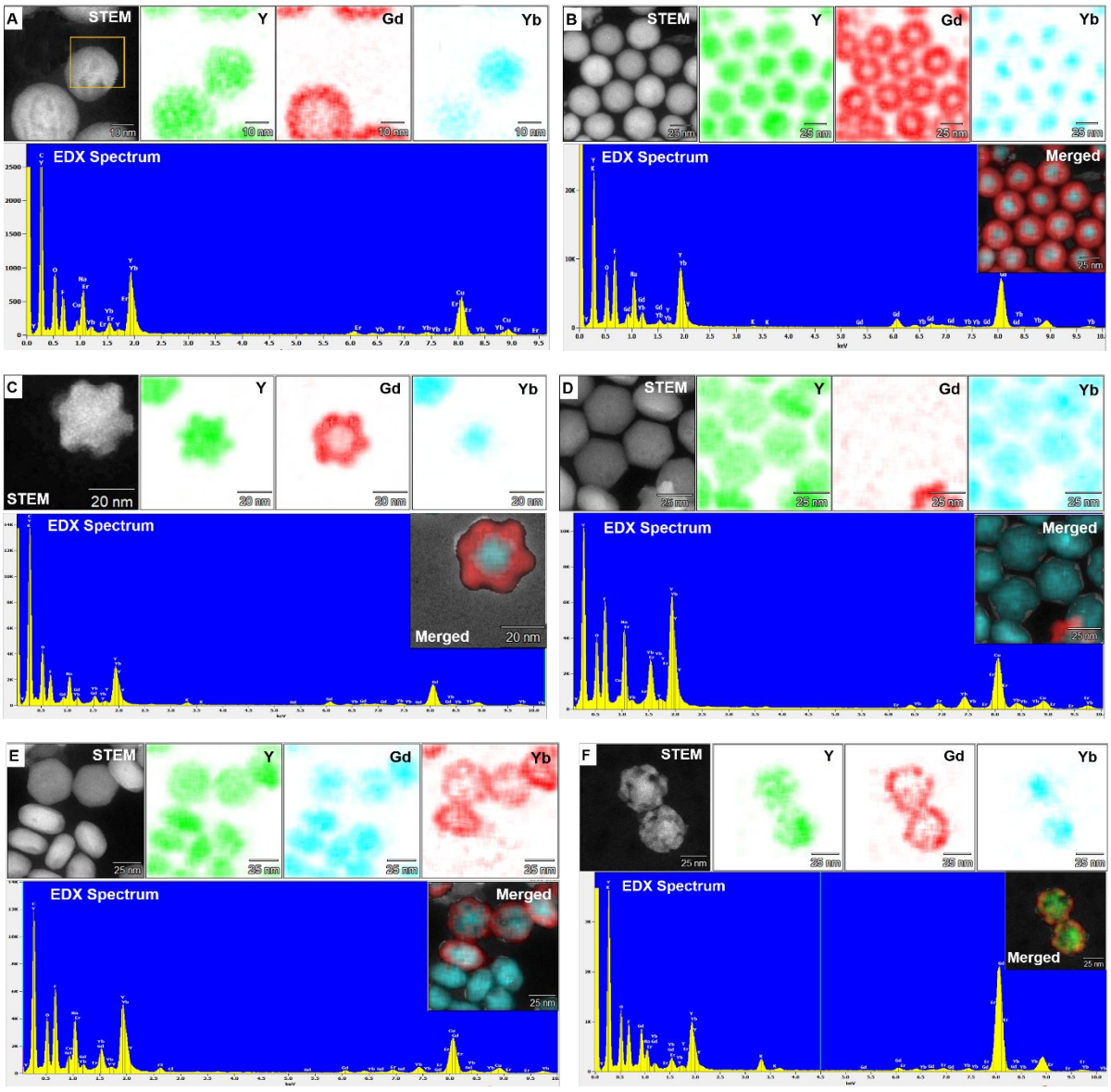

Figure S1. Detailed composition analysis with elemental mapping of Y^{3+}, Gd^{3+} and Yb^{3+} and EDX spectra for small core (A), core-shell (B), core-porous shell (C) UCNPs and large core (D), core-shell (E) and core-porous shell UCNPs.

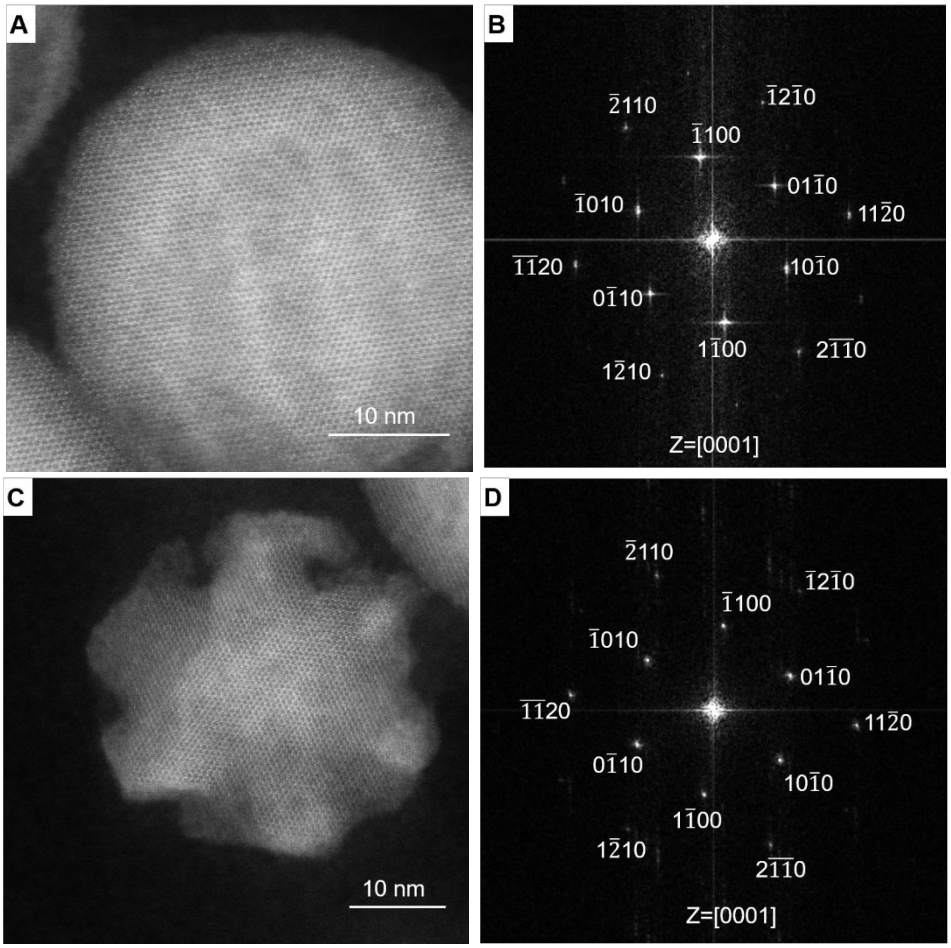

Figure S2. High Resolution TEM image (A) and Fast Fourier Transform image (B) of small core-shell UCNP and High-Resolution TEM image (C) and Fast Fourier Transform image (D) of small core-porous shell UCNP.

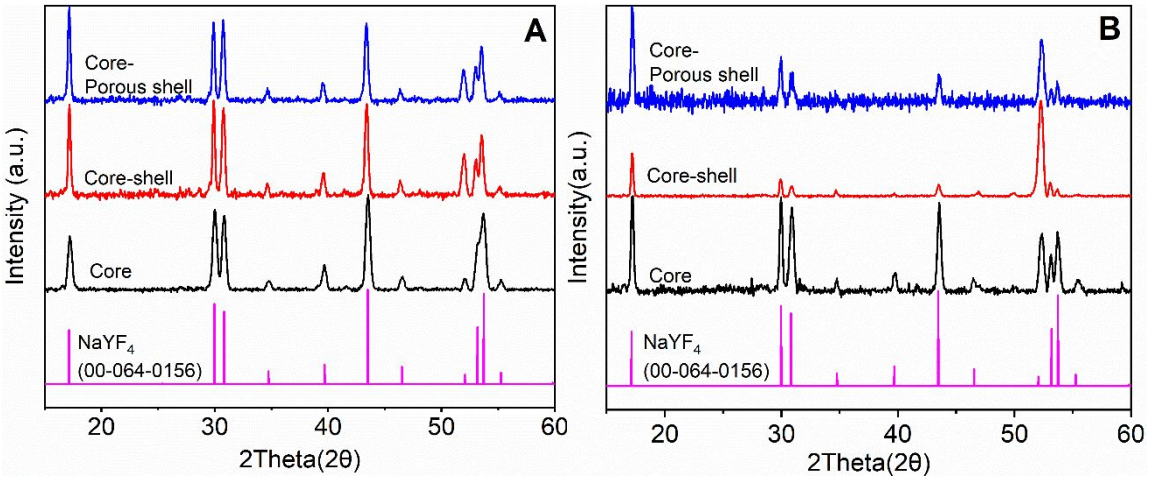

Figure S3. XRD patterns of small (A) and large (B) core, core-shell and core-porous shell UCNPs.

Table S1. Comparison of the MRI signal values of UCNPs.

Materials	Size (nm)	R1 (mM^{-1} s^{-1})	R2 (mM^{-1} s^{-1})	Magnetic Field (T)	Ref
D-glucuronic acid coated Gd_2O_3	1-2.5	9.9	10.5	3	9
PVP-$NaGdF_4$	2.5-8	3-7.2	-	1.5	10
$NaGdF_4$:Yb, Er-$NaGdF_4$:Nd-Sodium gluconate	26	5.73	-	3	11
$BaGdF_5$:5%Eu	40	0.59	2.88-4.88	1.5	12
$BaGdF_5$:0.5%Nd		0.93	3.52-3.78		
Ba_2GdF_7:Yb, Er-PEG	24±5	2.44	-	1.5	13
$NaGdF_4$-$CaCO_3$-PEG	~10	0.42	1.64	0.5	14
$NaGdF_4$: Yb, Tm	<5	3.37		1.4	5
pp-$NaGdF_4$	17.3	7.001	-	0.5	15
D-glucuronic acid coated Dy_2O_3 nanoparticles	3.2	negligible	65.04	1.5	16
	D=20, L=300	negligible	181.57	1.5	
Fe_3O_4, $ZnFe_2O_4$, $NiFe_2O_4$	4	5.991, 7.928, 6.850	15.534, 14.642, 12.921	1.5	17

REFERENCES

(1) Liu, D.; Xu, X.; Du, Y.; Qin, X.; Zhang, Y.; Ma, C.; Wen, S.; Ren, W.; Goldys, E. M.; Piper, J. A.; Dou, S.; Liu, X.; Jin, D., Three-dimensional controlled growth of monodisperse sub-50 nm heterogeneous nanocrystals. *Nat. Comm.* **2016**, *7*, 10254-10264.

(2) Ma, C.; Xu, X.; Wang, F.; Zhou, Z.; Wen, S.; Liu, D.; Fang, J.; Lang, C. I.; Jin, D., Probing the Interior Crystal Quality in the Development of More Efficient and Smaller Upconversion Nanoparticles. *J. Phys. Chem. Letters* **2016**, *7*, 3252-3258.

(3) Xu, X.; Zhou, Z.; Liu, Y.; Wen, S.; Guo, Z.; Gao, L.; Wang, F., Optimising passivation shell thickness of single upconversion nanoparticles using a time-resolved spectrometer. *APL Photonics* **2019**, *4*, 026104-026108.

(4) Fabricius, A.-L.; Duester, L.; Meermann, B.; Ternes, T. A., ICP-MS-based characterization of inorganic nanoparticles—sample preparation and off-line fractionation strategies. *Anal. Bioanal. Chem*. **2014**, *406*, 467-479.

(5) Naccache, R.; Chevallier, P.; Lagueux, J.; Gossuin, Y.; Laurent, S.; Vander Elst, L.; Chilian, C.; Capobianco, J. A.; Fortin, M.-A., High Relaxivities and Strong Vascular Signal Enhancement for NaGdF4 Nanoparticles Designed for Dual MR/Optical Imaging. *Adv. Healthc. Mater.* **2013**, *2*, 1478-1488.

(6) Vold, R. L.; Waugh, J. S.; Klein, M. P.; Phelps, D. E., Measurement of spin relaxation in complex systems. *J. Chem. Phys.* **1968**, *48*, 3831.

(7) Carr, H. Y.; Purcell, E. M., Effects of diffusion on free precession in nuclear magnetic resonance experiments. *Phys. Rev.* **1954**, *94*, 630.

(8) Meiboom, S.; Gill, D., Modified spin echo method for measuring nuclear relaxation times. *Rev. Sci. Instrum.* **1958**, *29*, 688-691.

(9) Park, J. Y.; Baek, M. J.; Choi, E. S.; Woo, S.; Kim, J. H.; Kim, T. J.; Jung, J. C.; Chae, K. S.; Chang, Y.; Lee, G. H., Paramagnetic Ultrasmall Gadolinium Oxide Nanoparticles as Advanced T1 MRI Contrast Agent: Account for Large Longitudinal Relaxivity, Optimal Particle Diameter, and In Vivo T1 MR Images. *ACS Nano* **2009**, *3*, 3663-3669.

(10) Johnson, N. J. J.; Oakden, W.; Stanisz, G. J.; Scott Prosser, R.; van Veggel, F. C. J. M., Size-Tunable, Ultrasmall NaGdF4 Nanoparticles: Insights into Their T1 MRI Contrast Enhancement. *Chem. Mater.* **2011**, *23*, 3714-3722.

(11) Ma, D.; Meng, L.; Chen, Y.; Hu, M.; Chen, Y.; Huang, C.; Shang, J.; Wang, R.; Guo, Y.; Yang, J., $NaGdF_4:Yb^{3+}/Er^{3+}@NaGdF_4:Nd^{3+}$@Sodium-Gluconate: Multifunctional and Biocompatible Ultrasmall Core–Shell Nanohybrids for UCL/MR/CT Multimodal Imaging. *ACS Applied Materials & Interfaces* **2015**, *7* (30), 16257-16265.

(12) Becerro, A. I.; González-Mancebo, D.; Cantelar, E.; Cussó, F.; Stepien, G.; de la Fuente, J. M.; Ocaña, M., Ligand-Free Synthesis of Tunable Size Ln:BaGdF5 (Ln = Eu^{3+} and Nd^{3+}) Nanoparticles: Luminescence, Magnetic Properties, and Biocompatibility. *Langmuir* **2016**, *32*, 411-420.

(13) Feng, Y.; Chen, H.; Ma, L.; Shao, B.; Zhao, S.; Wang, Z.; You, H., Surfactant-Free Aqueous Synthesis of Novel $Ba_2GdF_7:Yb^{3+}$, Er^{3+}@PEG Upconversion Nanoparticles for in Vivo Trimodality Imaging. *ACS App. Mater. Inter.* **2017**, *9*, 15096-15102.

(14) Wei, Z.; Lin, X.; Wu, M.; Zhao, B.; Lin, R.; Zhang, D.; Zhang, Y.; Liu, G.; Liu, X.; Liu, J., Core-shell $NaGdF_4@CaCO_3$ nanoparticles for enhanced magnetic resonance/ultrasonic dual-modal imaging via tumor acidic micro-enviroment triggering. *Sci. Rep.* **2017**, *7*, 5370-5370.

(15) Liu, K.; Dong, L.; Xu, Y.; Yan, X.; Li, F.; Lu, Y.; Tao, W.; Peng, H.; Wu, Y.; Su, Y.; Ling, D.; He, T.; Qian, H.; Yu, S.-H., Stable gadolinium based nanoscale lyophilized injection for enhanced MR angiography with efficient renal clearance. *Biomaterials* **2018**, *158*, 74-85.

(16) Kattel, K.; Park, J. Y.; Xu, W.; Kim, H. G.; Lee, E. J.; Bony, B. A.; Heo, W. C.; Jin, S.; Baeck, J. S.; Chang, Y.; Kim, T. J.; Bae, J. E.; Chae, K. S.; Lee, G. H., Paramagnetic dysprosium oxide nanoparticles and dysprosium hydroxide nanorods as T2 MRI contrast agents. *Biomaterials* **2012**, *33*, 3254-3261.

(17) Zeng, L.; Ren, W.; Zheng, J.; Cui, P.; Wu, A., Ultrasmall water-soluble metal-iron oxide nanoparticles as T1-weighted contrast agents for magnetic resonance imaging. *Physical Chemistry Chemical Physics* **2012**, *14*, 2631-2636.